

Supplemental material: acquiring axially-symmetric transparent objects using single-view transmission imaging

Jaewon Kim Ilya Reshetouski Abhijeet Ghosh
Imperial College London
{jaewon.kim15, ghosh}@imperial.ac.uk

1. Additional reconstruction results

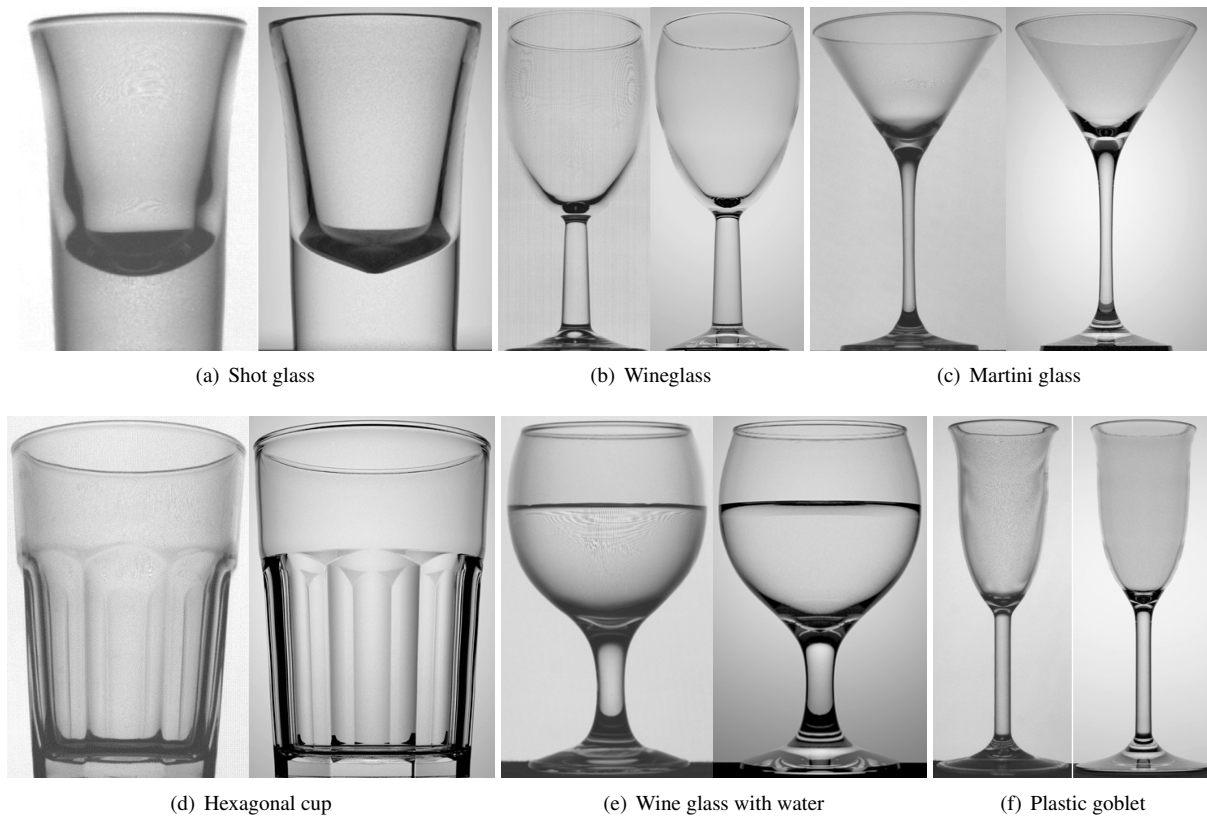


Figure 1: Reconstruction results for various axially transparent glass (a - e), and plastic (f) objects. Left: Photographs. Right: Renderings. (d) shows an n-fold symmetric tumbler. (e) shows a wine glass containing water.

Figure 1 presents a few additional reconstruction results to supplement those presented in the paper, including an n-fold symmetric example of a hexagonal cup (d). (a) presents an empty shot glass which can be compared to the reconstruction of the shot glass containing vodka in the paper (Fig. 13, e). While the inner walls of the glass are clearly visible in the empty shot glass, they are not visible in the glass containing vodka due to strong refraction inside the liquid volume. Such

distinct features are faithfully reflected in our reconstruction. (e) presents a wine glass containing water which can also be compared to the empty winglass shown in the paper (Fig. 8). Our reconstruction results are very close to the corresponding reference photographs demonstrating the accuracy of inner geometry and refractive index estimation in both cases. There are some minor noticeable differences in the reconstruction compared to the photographs along the inner boundaries in some sections of high curvature. This is mostly due to insufficient observations of ray deflection along these boundaries from a single viewpoint. (f) shows the result for a plastic goblet for which the refractive index estimation is presented in Fig. 7 in the paper. Generally, such plastic objects have more irregular shape than glass objects due to cheap and imprecise manufacturing process. The top hollow section of the plastic goblet in (f) is somewhat irregular as seen in the photograph. Since our method assumes complete rotational symmetry in this case, such irregularity cannot be reconstructed in the rendering result.

2. Refractive index estimation of liquids

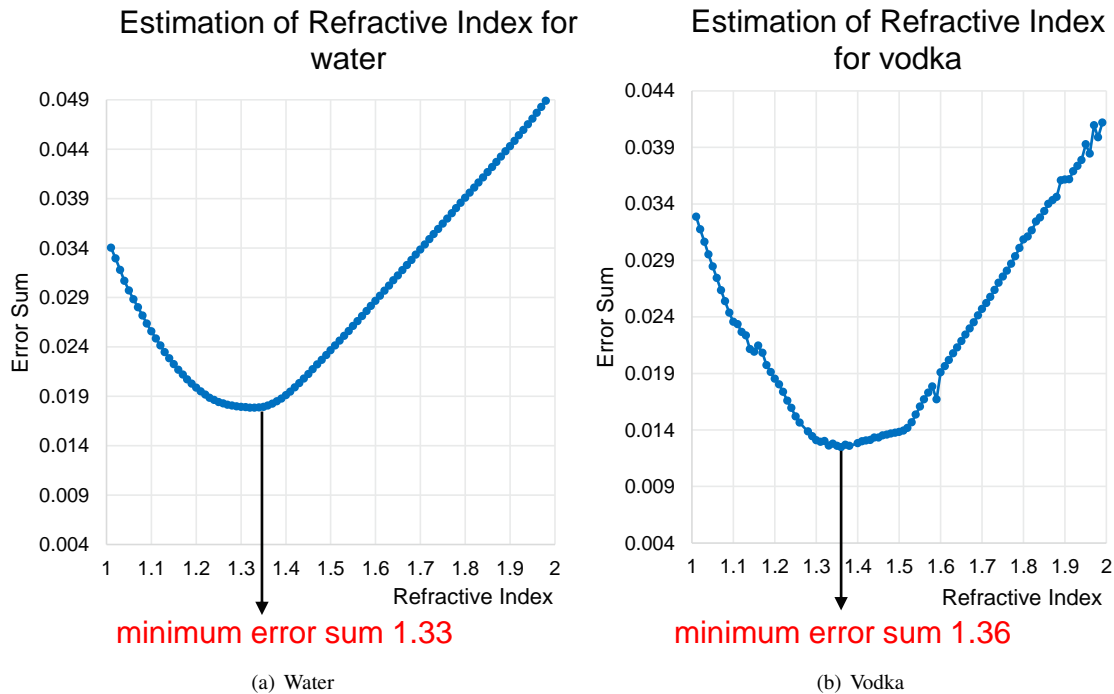



Figure 2: Refractive index estimation for water and vodka.

To estimate the refractive index of a liquid inside a transparent container, first outer and inner geometry and refractive index of the container are estimated by acquiring the empty container. Thereafter, the capture process is repeated with the liquid inside the container and inverse raytracing is employed to estimate the liquid’s refractive index. The estimated refractive index values for water (1.33) and vodka (1.36) with the above process correspond well to known values ¹.

¹https://help.thefoundry.co.uk/modo/901/content/help/pages/shading_lighting/shader_items/refract_index.html

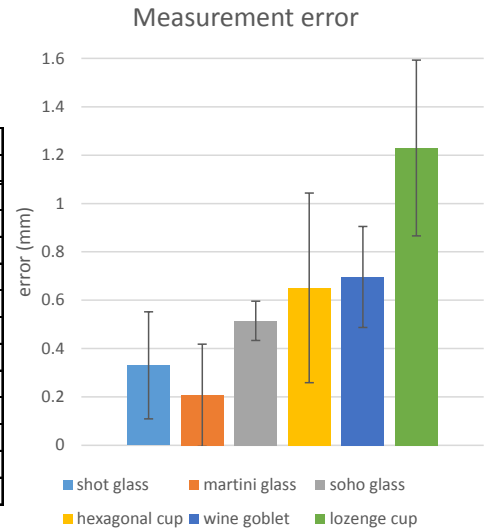
3. Vernier caliper measurements



Position \ Glasses	shot glass		martini glass		soho glass		hexagonal cup		wine goblet		lozenge cup	
	Meas.	Est.	Meas.	Est.	Meas.	Est.	Meas.	Est.	Meas.	Est.	Meas.	Est.
1	2.95	3.05	1.41	1.92	1.45	0.80	2.70	3.39	3.97	3.54	4.04	3.65
2	3.39	3.32	1.47	0.78	1.39	0.84	2.82	2.94	3.93	3.51	4.60	3.57
3	3.76	3.41	1.76	1.85	1.49	0.88	2.96	2.96	4.05	3.52	4.91	3.57
4	4.06	3.50	1.61	1.83	1.54	0.92	2.92	3.00	4.14	3.52	4.91	3.57
5	4.35	3.68	1.94	1.83	1.43	0.95	3.96	2.98	4.17	3.52	5.11	3.54
6	2.84	3.04	1.98	1.83	1.50	1.00	3.87	2.97	4.26	3.52	5.06	3.55
7	3.30	3.31	1.83	1.82	1.45	1.02	3.86	2.95	4.13	3.49	5.07	3.56
8	3.70	3.41	1.93	1.82	1.50	1.02	3.93	2.93	4.45	3.49	5.17	3.56
9	3.94	3.48	1.97	1.82	1.41	1.01	3.82	2.94	4.52	3.50	4.46	3.61
10	4.15	3.57	1.83	1.82	1.42	0.98	4.01	3.05	4.46	3.50	4.73	3.57
Avg. Error	0.33		0.21		0.51		0.65		0.70		1.23	
St. Dev	0.22		0.21		0.08		0.39		0.21		0.36	

(unit: mm)

(a) Measurement table



(b) Error graph with standard deviation

Figure 3: Measurement data to quantify our reconstruction accuracy.

In order to quantify our reconstruction accuracy, we measured 10 positions along the hollow sections of six different glass objects using a high precision vernier caliper (10 micron resolution). Height and wall thickness were measured at each position. We looked up the wall thickness at the same height in our reconstructed model for comparison. Half of the objects (shot, martini, and soho glass) are categorized as rotationally symmetric and the remainder (hexagonal cup, wine goblet, and lozenge cup) are n-fold symmetric. According to the caliper measurements, our method achieved slightly better accuracy for rotationally symmetric objects. We attribute this to the more complex shapes of the n-fold symmetric objects. Also, there is higher possibility of measurement errors for n-fold symmetric objects because they have complex outer geometry which makes accurate caliper measurements more difficult (e.g., the lozenge cup).

4. Mesh visualization of an n-fold symmetric object

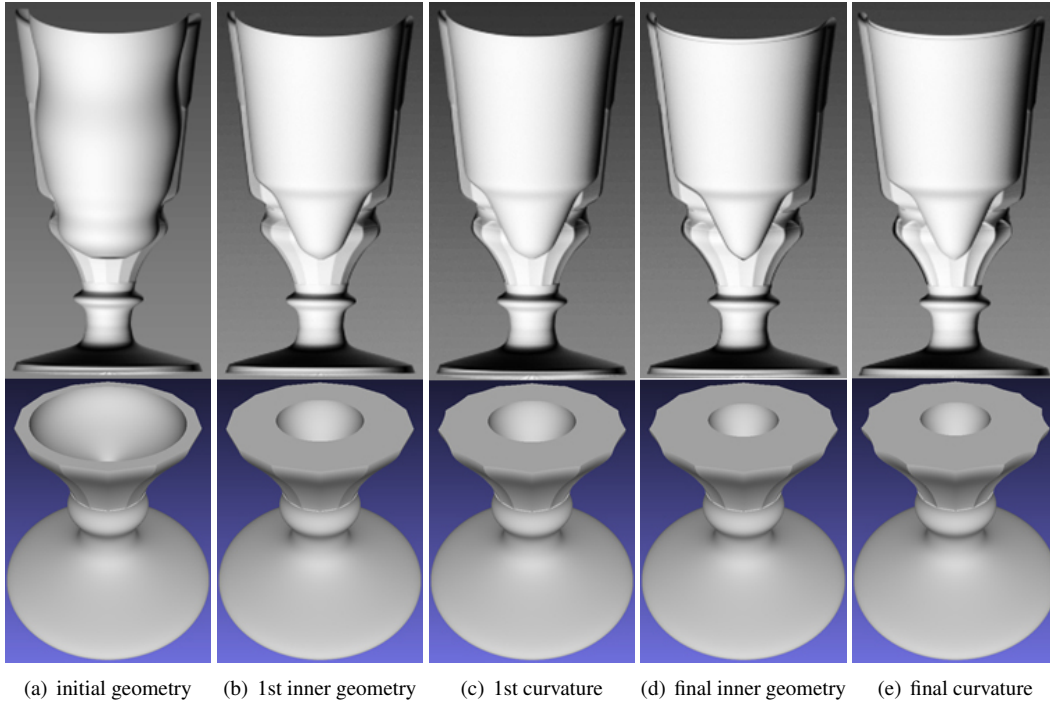


Figure 4: Mesh data visualization for the n-fold symmetric wine goblet presented in Fig.12 of the paper. From left to right, the inner geometry and outer curvature is iteratively refined until convergence.

Figure 4 shows sliced mesh visualization for the estimated geometry of the n-fold symmetric goblet shown in Fig. 12 in the paper. The mesh data clearly shows refinement of inner geometry and outer curvature with iterative estimation. (a) represents the initial geometry extracted using image processing. The inner geometry is far from the actual shape and the outer shape does not have any curvature for the faces. (b) and (c) show the first refinement of inner geometry and outer curvature respectively in a sequential manner. (d) and (e) is the final estimation of inner geometry and curvature which closely approximates the actual shape of the goblet.